IOP Conf. Series: Materials Science and Engineering **307** (2018) 012027 doi:10.1088/1757-899X/307/1/012027

Study of the nanoporous CHAP photoluminiscence for developing the precise methods of early caries detection

D Goloshchapov[1], P Seredin[1], D Minakov[2] and E Domashevskaya[1]

[1]Department of Solid State Physics and Nanostructures,Voronezh State University, Voronezh, Russia
[2]Department of Physical and Mathematical Sciences,Voronezh State University, Voronezh, Russia

E-mail: goloshchapov@phys.vsu.ru

Abstract. This paper deals with the luminescence characteristics of an analogue of the mineral component of dental enamel of the nanocrystalline **B**-type carbonate-substituted hydroxyapatite (CHAP) with 3D defects (i.e. nanopores of ~2-5 nm) on the nanocrystalline surface. The laser-induced luminescence of the synthesized CHAP samples was in the range of ~515 nm (~2.4 eV) and is due to CO_3 groups replacing the PO_4 group. It was found that the intensity of the luminescence of the CHAP is caused by structurally incorporated CO_3 groups in the HAP structure. Furthermore, the intensity of the luminescence also decreases as the number of the above intracentre defects (CO_3) in the apatite structure declines. These results are potentially promising for developing the foundations for precise methods for the early detection of caries in human solid dental tissue.

1. Introduction

Calcium hydroxyapatite (HAP) - $Ca_{10}(PO_4)_6(OH)_2$ and its substituted forms are the major biomineral component of bone tissue, enamel and dentine of human teeth as well as prosthesis material [1]. It is becoming increasingly important to develop methods (like laser-induced luminescence (PL)) for detecting pathologies of dental enamel at the outset of their development [2,3] and thus, analysing the overall condition of the bioapatite of dental enamel. It is well-known that as people age, calcium hydroxyapatite in the dental enamel transforms to carbonate-substituted calcium hydroxyapatite (CHAP) with many impurities [4,5], leading to additional risk of caries. It has been repeatedly shown [6] that healthy, affected and caries-damaged areas have a displacement as well as additional bands in the photoluminescence spectra. This helps to visualize the PL signal and map the affected area or the oral cavity, indicating overall changes in colour from pathogenic areas. Thus, lately there have been many methods developed and a variety of tools employed for clinical use to estimate the photoluminescence signal from solid dental tissues [7,8].

Regarding the luminescence of solid dental tissues, both the organic and mineral components contribute to their photoluminescence spectrum [2]. Moreover, the type of defect in the structure of calcium hydroxyapatite can be crucial to the luminescence maximum [9]. In addition to intracentre defects, changes in the bioapatite photoluminescence spectrum can be caused by a variety of phase transformations occurring leading up to caries development in human enamel and dentine [10].

Unfortunately, as yet, modern methods are incapable of detecting such pathologies in solid dental tissue (caries) at an early stage and along its depth, due to the signal being difficult to detect at the level of intralattice replacements in a crystal lattice of an apatite and molecular local atomic

surroundings (different impurities in the composition). However, addressing the synthesis of composite biomimetic materials similar to dental tissues (intact and caries-damaged) in their composition, as well as further analysis of their photoluminescence will assist in finding more effective approaches for the early detection of local areas of intact enamel and caries-damage and, more importantly, in making these tools more sensitive [7,11].

Therefore, the objective of the paper is to study emission properties of analogues of the mineral component of native dental tissue, i.e. carbonate-substituted nanocrystaline hydroxyapatite, and to identify the dependences of spectral characteristics of synthesized biomaterials on the amount of impurities in them.

2. Materials and research methods

In this study, nanocrystalline carbonate-substituted hydroxyapatite was obtained using egg shells by means of the our method detailed previously [12]. Changes in the concentration of carbonate-containing groups was controlled using a pH from 9 to 7, with a step of 0.5 (pH-meter/ionometer IPL 111-1) and accuracy of 0.01 as in [13].

The samples of hydroxyapatite were investigated by X-ray diffraction (DRON-4.07 Co Kα = 1,790Å), Fourier infrared spectroscopy (Vertex-70, Bruker), Raman scattering spectroscopy (LabRam HR800), transmission electron microscopy (Libra-120 Carl Zeiss) and photoluminescence spectroscopy (a setup based on fibre optics spectrometer USB4000-VIS-NIR by OceanOptics) and a laser excitation source with the wavelength of 405 nm.

3. Results and discussion

The results of X-ray diffraction showed that the materials are nanocrystalline forms of hydroxyapatite, with an average crystallite size of 35 nm according to [12]. In order to specify the local microstructure and phase constancy of the samples, high-resolution transmission electron microscopy was employed (Fig. 1).

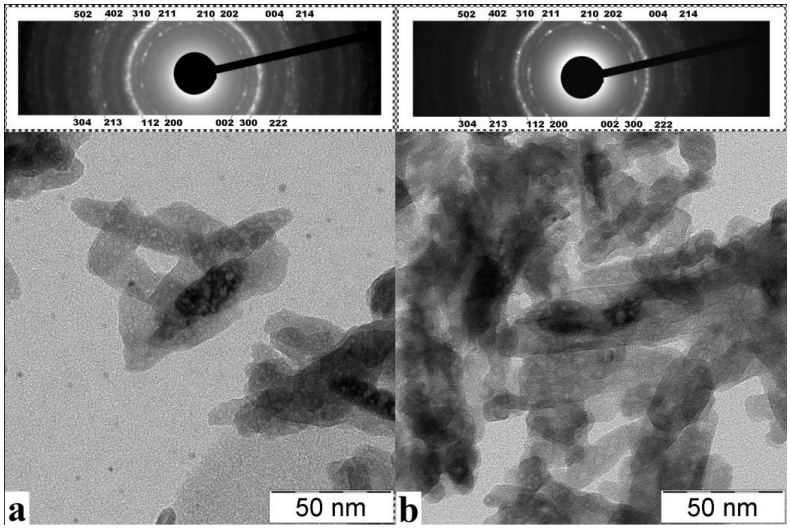

Fig. 1: Transmission electron microscopy of a microphotograph and microdiffraction of the samples obtained using the solution of a) pH = 9 and b) pH = 7.

The study of morphology of hydroxyapatite nanocrystals using nanometer resolution transmission electron microscopy showed the presence of nanocrystals with a defective porous structure on the surface (Fig. 1). The presented microphotographs suggest that as the pH of the solution decreases, the size of the nanopores increases.

IR-spectroscopy revealed that all the samples are carbonate-substituted forms of hydroxyapatite. The vibration modes in the IR-spectra at 1415 cm^{-1}, 1425 cm^{-1} and 1450 cm^{-1} indicate CHAP of B-type, that is, replacement of PO_4 group with CO_3 group as shown previously in [12,13]. The experimental data showed that in the samples investigated for the current study, the intensity of the

vibration modes of CO_3 group in the IR-spectra decreases from sample to sample, while that of the major mode of PO_4 group remains unchanged. This fact refer to degree of replacement of the PO_4 group by CO_3 in the structure of apatite [13,14]. At the stage of the synthesis of the samples, as the pH of the solution decreases from 9 to 7 (introduction of a large number of PO_4 groups), so does the intensity of the vibration mode of the carbonate-anion included in the hydroxyapatite structure.

Studies of calcium hydroxyapatite suggest that when there are displacements in the apatite crystal lattice and a CO_3 anion is included in the hydroxyapatite structure, there is a shift in PO_4 bands in the spectra of Raman scattering spectroscopy. Raman spectroscopy was performed to identify the influence of a defect in the structure of the synthesized samples of calcium hydroxyapatite on their optical properties (see Fig. 2).

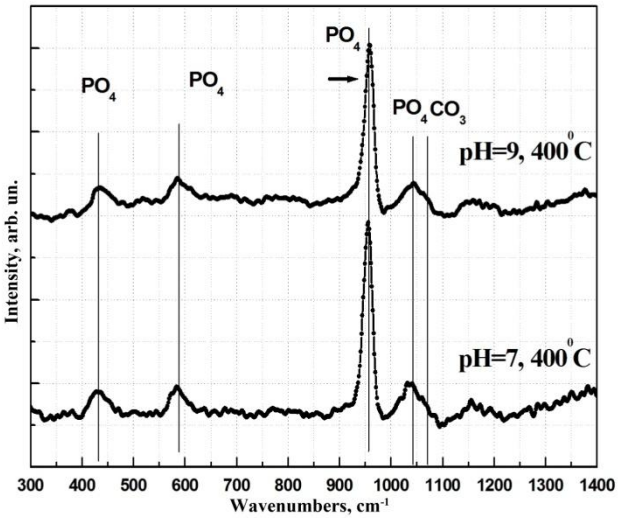

Fig. 2: Raman spectra of the samples with pH 9 and 7 annealed at 400°C.

As seen in Figure 2, except for the major modes of the phosphorus-oxygen group identified at around 961, 587 and 431 cm^{-1}, in the spectra of the samples from different pH solutions, there is an additional mode in the area of ~1070 cm^{-1}. It might be due to the carbonate anion CO_3^{2-} in the structure of calcium hydroxyapatite that replaced PO_4^{3-} in the lattice. Note that in this spectrum range, 1077, 1045, 1035 cm^{-1}, there are low-intensive modes of PO_4 group. It should also be mentioned that the ratio of the intensities of additional modes and the major phosphate mode identified at around 961 cm^{-1} in all the spectra remains identical. A detailed study of the form of the vibration of PO_4 (Fig. 2) showed that the inclusion of the CO_3 anion into the structure of hydroxyapatite caused asymmetries and a shift of the maximum by 5 cm^{-1} for the samples with pH values of 7 and 9. This correlates with the IR-spectroscopy data on the nature of carbonate-substituted samples of B-type CHAP.

Photoluminescence spectroscopy of the samples revealed a strong dependence of the intensity of the major photoluminescence maximum on the conditions of obtaining materials (CHAP), by means of the suggested method as well as on their subsequent thermal processing. Fig. 3a shows the photoluminescence spectra of all the samples of calcium hydroxyapatite obtained in this study for different (final) pH values (9, 8.5, 8, 7.5, 7) and annealed at 400°C. The maximum of the photoluminescence band is in the range of ~515 nm, corresponding with the transition energy of ~2.4 eV. The analysis of the spectra of CHAP showed that the photoluminescence intensity of the samples with a pH of 7.5 and 7 is lower than that of the samples with a pH of 9-8. This might be caused by a decrease in the concentration of the impurity luminescence centres of CO_3^{2-} in the samples obtained for smaller values of pH. The ratios of the intensities in the profile of the photoluminescence bands might be due to the element composition of the original material (egg shells) that was used to synthesize hydroxyapatite. In synthesized materials, the maximum concentration of the carbonate anion is ~5%, what is comparable with their content in the bioapatite of human dental enamel [15]. Comparing the method of synthesis described in our previous paper [12] and the data of similar

studies, it appears that obtaining hydroxyapatite by means of liquid-phase methods leads to inclusion of the atmospheric gas CO_2 in the resultant material, resulting in fluctuations in the carbonate anion content, thereby rendering the photoluminescence bands of the specified intensity particularly important for observations.

An analysis of the literature shows that photoluminescence in pure hydroxyapatite might be caused by structural defects occurring as a result of intentional or random modifications of the composition [16,17].

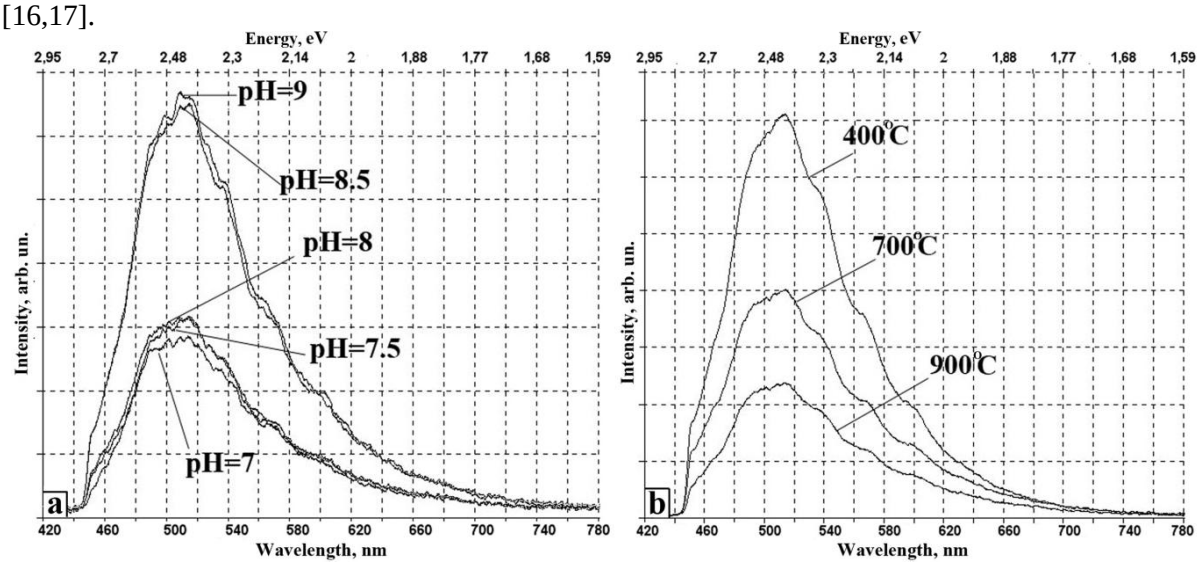

Fig. 3. Photoluminescence spectra of calcium hydroxyapatite: a - obtained at pH values of 9, 8.5, 8, 7.5, 7 and annealed at 400°C; b - with a pH = 8.5 and annealed at 400, 700, 900°C.

In [9], there are results of a study of own photoluminescence of hydroxyapatite according to which its forbidden band width is ~7,7 eV. Using this value and the obtained photoluminescence spectra with the maximum ~2.4eV (Fig. 3a), we consider a possible variant of a model of photoluminescence of carbonate-substituted hydroxyapatite whose center of luminescence is CO_3 group replacing PO_4 group in the structure of calcium hydroxyapatite. Note that in [9] the photoluminescence maximum that depends on own defects of pure hydroxyapatite was measured at ~3,8 eV. However, the energy of the source of excitation that we used does not allow photoluminescence to be observed at such energies, thus the measured laws for the intracenter photoluminescence with a maximum at ~2.4 eV.

The PL investigation of the calcium hydroxyapatite samples exposed to thermal annealing in the temperature range of 400-900°C proved the relatively impurity mechanism (intracentre defects CO_3) of the observed photoluminescence. The photoluminescence of the samples obtained at the same pH (8.5), but annealed at 400, 700, 900°C decreased as the temperature increased (Fig. 3b), due to a reduction in the carbonate ion content of the calcium hydroxyapatite. This is in good agreement with the results obtained by means of X-ray structure analysis and IR-spectroscopy, and does not contradict the photoluminescence model being investigated.

4. Conclusion

This paper investigated the luminescence characteristics of synthesized samples of carbonate-substituted hydroxyapatite of B-type (calcium-deficient hydroxyapatite), i.e. an analogue of the mineral component of dental enamel. Using the methods of X-ray diffraction and transmission electron microscopy, all the synthesized samples were confirmed as nanocrystalline calcium hydroxyapatite, with nanopores on the surface of nanocrystals. IR and Raman spectroscopy indicated that the PO_4 group was replaced by a CO_3 group during synthesis of the obtained materials. The study of the luminescence properties of the synthesized samples showed that they have a maximum luminescence at ~515 nm (~2.4 eV). The comparison of the luminescence spectra revealed that changes in the pH of the solution used in the synthesis of calcium hydroxyapatite influenced the

intensity of the photoluminescence, possibly due to fewer CO_3^{2-} groups in the calcium hydroxyapatite structure obtained at a lower pH. Furthermore, the features of the photoluminescence spectra can be utilized in the development of precise methods for the early detection of caries in human solid dental tissue.

Acknowledgments
This work was supported by the grant of Russian Science Foundation, grant number 17-75-10046.

References
[1] Dorozhkin S V 2017 *Hydroxyapatite and Other Calcium Orthophosphates: Bioceramics, Coatings and Dental Applications [Hardcover]* (Nova Science Publishers, Inc New York)
[2] Seredin P V, Goloshchapov D L, Kashkarov V M, Ippolitov Y A and Prutskij T 2016 Emission properties of biomimetic composites for dentistry *Results Phys.* **6** 447–8
[3] Rocha-Cabral R M, Mendes F M, Maldonado E P and Zezell D M 2015 A simple dental caries detection system using full spectrum of laser-induced fluorescence ed C Kurachi, K Svanberg, B J Tromberg and V S Bagnato p 95311A–1–95311A–13
[4] Leventouri T, Antonakos A, Kyriacou A, Venturelli R, Liarokapis E and Perdikatsis V 2009 Crystal Structure Studies of Human Dental Apatite as a Function of Age *Int. J. Biomater.* **2009** 1–6
[5] Piga G, Goncalves D, Thompson T J U, Brunetti A, Malgosa A and Enzo S 2016 Understanding the Crystallinity Indices Behavior of Burned Bones and Teeth by ATR-IR and XRD in the Presence of Bioapatite Mixed with Other Phosphate and Carbonate Phases *Int. J. Spectrosc.* **2016** 1–9
[6] Chen Q G, Zhu H H, Xu Y, Lin B and Chen H 2015 Quantitative method to assess caries via fluorescence imaging from the perspective of autofluorescence spectral analysis *Laser Phys.* **25** 085601
[7] Panayotov I, Terrer E, Salehi H, Tassery H, Yachouh J, Cuisinier F J G and Levallois B 2012 In vitro investigation of fluorescence of carious dentin observed with a Soprolife® camera *Clin. Oral Investig.* **17** 757–63
[8] Sarycheva I, Yanushevich O, Minakov D and Shulgin V 2015 Fluorescence of intact human teeth enamel in vivo *J. Stomatol.* **68** 424–9
[9] Feldbach E, Kirm M, Kotlov H and Mägi H Luminescence Spectroscopy of Ca-apatites under VUV Excitation *DESY Photon Sci. Annu. Rep.*
[10] Bachmann L, Zezell D M, Ribeiro A da C, Gomes L and Ito A S 2006 Fluorescence Spectroscopy of Biological Tissues—A Review *Appl. Spectrosc. Rev.* **41** 575–90
[11] Seredin P V, Goloshchapov D L, Prutskij T and Ippolitov Y A 2017 Fabrication and characterisation of composites materials similar optically and in composition to native dental tissues *Results Phys.* **7** 1086–94
[12] Goloshchapov D L, Kashkarov V M, Rumyantseva N A, Seredin P V, Lenshin A S, Agapov B L and Domashevskaya E P 2013 Synthesis of nanocrystalline hydroxyapatite by precipitation using hen's eggshell *Ceram. Int.* **39** 4539–49
[13] Yusufoglu Y and Akinc M 2008 Effect of pH on the Carbonate Incorporation into the Hydroxyapatite Prepared by an Oxidative Decomposition of Calcium–EDTA Chelate *J. Am. Ceram. Soc.* **91** 77–82
[14] Komlev V S, Fadeeva I V, Gurin A N, Kovaleva E S, Smirnov V V, Gurin N A and Barinov S M 2009 Effect of the concentration of carbonate groups in a carbonate hydroxyapatite ceramic on its in vivo behavior *Inorg. Mater.* **45** 329–34
[15] Grunenwald A, Keyser C, Sautereau A M, Crubézy E, Ludes B and Drouet C 2014 Revisiting carbonate quantification in apatite (bio)minerals: a validated FTIR methodology *J. Archaeol. Sci.* **49** 134–41
[16] Liu J, Wu Q and Ding Y 2005 Self-Assembly and Fluorescent Modification of Hydroxyapatite Nanoribbon Spherulites *Eur. J. Inorg. Chem.* **2005** 4145–9
[17] Zhang C, Yang J, Quan Z, Yang P, Li C, Hou Z and Lin J 2009 Hydroxyapatite Nano- and Microcrystals with Multiform Morphologies: Controllable Synthesis and Luminescence Properties *Cryst. Growth Des.* **9** 2725–33